Science of the Total Environment 650 (2019) 1019–1028

Contents lists available at ScienceDirect

Science of the Total Environment

journal homepage: www.elsevier.com/locate/scitotenv

Biofilm and temperature controls on greenhouse gas (CO_2 and CH_4) emissions from a *Rhizophora* mangrove soil (New Caledonia)

Adrien Jacotot [a,b,*], Cyril Marchand [a], Michel Allenbach [b]

[a] IMPMC, Institut de Recherche pour le Developpement (IRD), UPMC, CNRS, MNHN, Noumea, New Caledonia, France
[b] Université de la Nouvelle-Calédonie, ISEA, EA 7484, BPR4, 98851 Noumea, New Caledonia

HIGHLIGHTS

- We measured soil CO_2 and CH_4 fluxes in a mangrove forest at low tide.
- Mean CO_2 and CH_4 emissions were 91.70 mmol m^{-2} day^{-1} and 117.30 μmol m^{-2} day^{-1}.
- CO_2 and CH_4 emissions were significantly higher during the warm season.
- Mean $\delta^{13}C\text{-}CO_2$ was −19.76 ± 1.19‰, showing a mixing between different sources.
- Biofilm development is a major driving factor of gas emissions to the atmosphere.

GRAPHICAL ABSTRACT

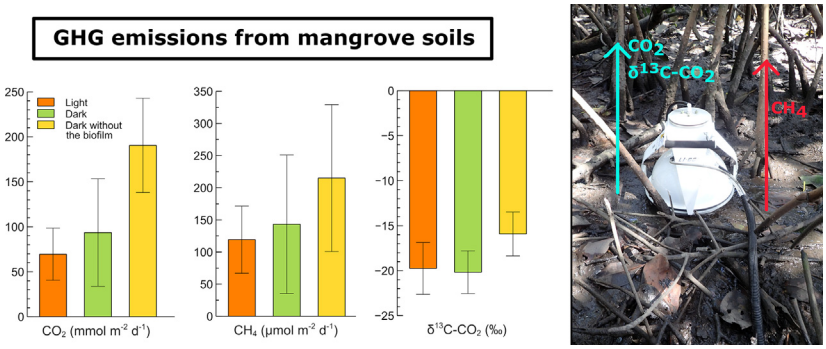

ARTICLE INFO

Article history:
Received 27 May 2018
Received in revised form 6 September 2018
Accepted 7 September 2018
Available online 8 September 2018

Editor: F.M. Tack

Keywords:
Soil fluxes
Greenhouse gas
Carbon stable isotopes
Biofilm
Blue carbon
Semi-arid mangrove

ABSTRACT

Seasonal variations of CO_2 and CH_4 fluxes were investigated in a *Rhizophora* mangrove forest that develops under a semi-arid climate, in New Caledonia. Fluxes were measured using closed incubation chambers connected to a CRDS analyzer. They were performed during low tide at light, in the dark, and in the dark after having removed the top 1–2 mm of soil, which may contain biofilm. CO_2 and CH_4 fluxes ranged from 31.34 to 187.48 mmol m^{-2} day^{-1} and from 39.36 to 428.09 μmol m^{-2} day^{-1}, respectively. Both CO_2 and CH_4 emissions showed a strong seasonal variability with higher fluxes measured during the warm season, due to an enhanced production of these two gases within the soil. Furthermore, CO_2 fluxes were higher in the dark than at light, evidencing photosynthetic processes at the soil surface and thus the role of biofilm in the regulation of greenhouse gas emissions from mangrove soils. The mean $\delta^{13}C\text{-}CO_2$ value of the CO_2 fluxes measured was −19.76 ± 1.19‰, which was depleted compared to the one emitted by root respiration (−22.32 ± 1.06‰), leaf litter decomposition (−21.43 ± 1.89‰) and organic matter degradation (−22.33 ± 1.82‰). This result confirmed the use of the CO_2 produced within the soil by the biofilm developing at its surface. After removing the top 1–2 mm of soil, both CO_2 and CH_4 fluxes increased. Enhancement of CH_4 fluxes suggests that biofilm may act as a physical barrier to the transfer of GHG from the soil to the atmosphere. However, the $\delta^{13}C\text{-}CO_2$ became more enriched, evidencing that the biofilm was not integrally removed, and that its partial removal resulted in physical disturbance that stimulated CO_2 production. Therefore, this study provides useful information to understand the global implication of mangroves in climate change mitigation.

1. Introduction

Anthropogenic emissions of greenhouse gases to the atmosphere increased significantly since preindustrial times to the point that current

* Corresponding author at: Institut de Recherche pour le Developpement, BPA5, 98848 Noumea, New Caledonia.
E-mail address: adrien.jacotot@protonmail.com (A. Jacotot).

https://doi.org/10.1016/j.scitotenv.2018.09.093
0048-9697/

emissions have reached their highest rates for the last 66 million years (Zeebe et al., 2016). As a result, atmospheric CO_2 concentrations are now at their highest level for the last 800,000 years (Lüthi et al., 2008). Despite the development of alternative energies to fossil fuels, the different projections for the end of the century do not show any decrease of the emissions. Therefore, there are urgent needs to evaluate the ability of natural ecosystems to fix and store carbon, which also includes the greenhouse gas emissions from these ecosystems, in order to adopt appropriate climate change mitigation programs such as ecosystems conservation and restoration strategies.

Mangroves are forested ecosystems that develop along tropical and subtropical coastlines, providing numerous ecosystems services (Barbier et al., 2011; Lee et al., 2014). Due to their high primary productivity, estimated to 218 ± 72 Tg C $year^{-1}$ (Bouillon et al., 2008), and their high carbon storage capacity, with up to 15% of their productivity being buried in their soils (Breithaupt et al., 2012), mangroves notably play a critical role in the coastal carbon cycle and were thus recently named "blue carbon" sinks (McLeod et al., 2011). Mangrove soils are mainly anoxic, limiting organic matter (OM) decay processes and thus greenhouse gas (GHG) production. However, due to their position between land and sea, mangroves are regularly flooded by tides, and their soils may alternate between suboxic and anoxic conditions, modifying GHG production and emissions (Allen et al., 2007; Chauhan et al., 2015; Chen et al., 2016a, 2016b; Oertel et al., 2016). In mangrove soils, the CO_2 produced derives mainly from biofilm respiration, roots respiration, leaf litter degradation, and organic matter decomposition (Kristensen et al., 2008). In contrast to CO_2 production, methanogenesis is a strictly anaerobic process that only occurs when all electron acceptors have been exhausted. Considering the inputs of sulfate during each tide, CH_4 emissions from mangrove forests may be low or non-existent (Alongi et al., 2004; Alongi et al., 2001). However, recent studies demonstrated that sulfate reduction and methanogenesis can coexist in mangrove soils due to the utilization of other non-competitive substrates by methanogens (Lyimo et al., 2002), and thus it was suggested that these CH_4 emissions may have been underestimated (Chauhan et al., 2015; Lyimo et al., 2002). CH_4 may notably be of major concern due to its global warming potential, 25 times higher than CO_2 over a 100 year time frame (Myhre et al., 2013). Nevertheless, there is still a paucity of research in this area, and the variability of greenhouse gas emissions from mangrove soils remains poorly understood, notably due to the number of parameters that have to be taken into account (*e.g.* mangrove species, latitude, anthropic pressure, *etc.*).

For a specific area, several environmental factors have been shown to influence the emissions of greenhouse gases to the atmosphere from mangrove soils, such as soil water content, organic matter content, or even salinity (Bulmer et al., 2015; Chanda et al., 2013; Chen et al., 2016b; Chen et al., 2014; Chen et al., 2012; Kirui et al., 2009; Leopold et al., 2015; Leopold et al., 2013; Livesley and Andrusiak, 2012; Poungparn et al., 2009). Seasonal changes in temperature is also an important parameter involved in the variability of greenhouse gas emissions, affecting the rates of soil organic matter decay, and thus GHG production and emissions (Barroso-Matos et al., 2012; Conant et al., 2011; Davidson and Janssens, 2006; Fang and Moncrieff, 2001; Fierer et al., 2005; Mackey and Smail, 1996). In addition, the development of biofilm at the sediment surface has been shown to be another major driving factor of GHG emissions from mangroves soils (Bulmer et al., 2015; Leopold et al., 2015; Leopold et al., 2013).

Furthermore, recent development of advanced technologies such as cavity ring-down spectroscopy (CRDS) allows high resolution *in situ* simultaneous measurements of both CO_2 and CH_4 fluxes, and also of $\delta^{13}C\text{-}CO_2$. These new analytical means could help to identify the origins of the CO_2 emitted from mangrove soils.

With this context, our main objectives were to: (i) quantify the CO_2 and CH_4 fluxes from the soil to the atmosphere, in the light and in the dark, during low tide within a *Rhizophora* spp. mangrove forest developing under semi-arid climate, (ii) evaluate the seasonal variability of the emissions, and (iii) identify the origin of the CO_2 fluxes measured. We hypothesized that fluxes will be higher during the warm season as a result of higher temperatures. Then, we further suggested that CO_2 fluxes will be lower in the light due to biofilm photosynthetic activity, which may consume CO_2. To reach our goals, we performed a one-year survey, with measurements every month, using incubation chambers connected to a CRDS analyzer. CO_2 and CH_4 fluxes were measured (i) at light with a transparent chamber, (ii), in the dark, with an opaque chamber, and (iii) in the dark after having removed the upper 1–2 mm of soil that may contain the biofilm. The CO_2-emitted isotopic value ($\delta^{13}C\text{-}CO_2$) was measured for each incubation, and the gases concentrations as well as the physicochemical parameters within the soil were also measured.

2. Material and methods

2.1. Site description

Field work was performed in the mangrove of Ouemo (22°16′50″S, 166°28′16″E), in New Caledonia, a French overseas archipelago located in the South Pacific, in the Melanesia sub region (21°21′S, 165°27′E). The archipelago sheltered 35,100 ha of mangroves, composed of 24 different species (Virly, 2006), however the studied mangrove was dominated by three *Rhizophora* mangrove species: *R. stylosa*, *R. samoensis* and *R. selala*. Climate in New Caledonia is strongly influenced by the variation of the inter-tropical convergence zone (ITCZ) that defines two contrasting seasons: a cool and dry season from May to September, and a warm cyclonic season from November to April. Average air temperature in Ouemo varied between 20.5 and 26.6 °C, with a mean annual precipitation of 1070 mm (data from meteofrance.com). The tidal regime in the region is semi-diurnal, with a tidal range ranging from 1.10 to 1.70 m.

2.2. Soil CO_2, $\delta^{13}C\text{-}CO_2$ and CH_4 emissions

Soil CO_2, $\delta^{13}C\text{-}CO_2$ and CH_4 emissions were measured using closed incubation chambers connected *via* PTFE gas tubes to a G2131-*i* CRDS analyzer (Picarro Inc., Santa Clara, CA, USA) that measures gas concentrations at a frequency of 1 Hz. An internal pump to the instrument (0.1 l min^{-1}) allowed the circulation of the air trapped inside the chamber through the system. Incubation chambers penetrated only a few millimeters into the sediment, which was sufficient to be airtight but not to damage the fine surface roots or sediment structure that could cause gas exchanges. Operational ranges of the analyzer are 100–4000 ppm for CO_2, and 0–1000 ppm for CH_4. Guaranteed precision by the manufacturer are for CO_2 concentrations (30 s measurement, 1-σ) 200 ppb (^{12}C) / 10 ppb (^{13}C), for CH_4 concentrations (30 s measurement,1-σ) 50 ppb + 0.05% of reading (^{12}C), and for $\delta^{13}CO_2$ (5 min measurement,1-σ) < 0.1‰ between 380 and 1000 ppm CO_2. Accuracy of the CRDS analyzer was periodically checked using certified N_2 (0 ppm CO_2 and CH_4), CO_2 (503 ppm) and CH_4 (100 ppm) gas standard samples (Calgaz, Air Liquide, USA).

Gas fluxes measurements were performed every month, from October 2016 to September 2017 for a total of 12 field campaign. Each month, one sunny day with a low tide occurring around noon was chosen. Measurements were conducted between 2 h prior and after low tide.

Firstly, triplicate incubations (6 min each) were made at light, using a transparent acrylic chamber (26 cm in diameter and 13 cm in height; 5122 cm^3) directly placed on the soil. Then, after 15 min of soil shading, measurements were performed in the dark, using an opaque acrylic chamber (20 cm in diameter and 13 cm in height; 4843 cm^3). Finally, the top 1–2 mm of soil that may contain the biofilm was carefully removed and stored for chlorophyll-*a* analyses, and three supplementary dark incubations were performed (Bulmer et al., 2015; Leopold et al., 2015). The above procedure was repeated three times during each

campaign of measurement. To avoid spatial variability, each complete measurement cycle (*i.e.* light, dark and dark after biofilm removal) was performed at a same sampling point, separated from the two others sampling points by a distance of ~1 m. In addition, the sampling positions were slightly modified each month to overcome an effect of biofilm removal during the last sampling campaign.

To characterize the isotopic value of the CO_2 sources, additional incubations on intact roots and leaf litter were also carried out, using specifics cylindrical opaque incubation chambers made with PVC pipe (203,97 cm^3). Measurements of roots and leaf litter isotopic values were performed in triplicate.

2.3. Flux calculations

CO_2 and CH_4 fluxes were calculated from the linear regression of the concentrations within the chamber over time, using the following equation:

$$F_{(CO2,CH4)} = (d(CO_2, CH_4)/dt) * V/(R * S*) * 86.4$$

where F is the fluxes of CO_2 or CH_4 ($\mu molC \cdot m^{-2}\ day^{-1}$); $d(CO_2, CH_4)/dt$ is the variation in CO_2 or CH_4 as a function of time ($ppm\ s^{-1}$); V is the total volume of the system (m^3); R is the ideal gas constant of 8.205746 10^{-5} ($atm \cdot m^3 \cdot K^{-1} \cdot mol^{-1}$); T is the absolute air temperature (K); S is the area of the bottom of the incubation chamber (m^2); and 86.4 is a conversion factor.

2.4. Isotopic CO_2 characterization

A Keeling plot approach was used to discriminate the isotopic value of the CO_2 ($\delta^{13}C\text{-}CO_2$) released from soil, roots respiration and leaf litter decomposition from the background atmosphere trapped inside the chambers (Keeling, 1961, 1958; Pataki et al., 2003). This approach is based upon mass conservation during the CO_2 exchange between two compartments. The intercept of the linear regression that describes the change in $\delta^{13}C\text{-}CO_2$ in function of the inverse of the CO_2 concentrations corresponds to the $\delta^{13}C\text{-}CO_2$ value of the CO_2 added to the chamber.

2.5. Soil CO_2 and CH_4 concentrations

Triplicate 60 cm deep cores were collected using a Eijkelkamp gouge auger (1 m long, 8 cm diameter) during each measurement campaigns at the exception of October 2016 and September 2016. Cores were taken at a distance of 20 m from the incubations area. They were separated in 6 subsections of 10 cm length, and pore-water was extracted from each section using Rhizon micro sampler (10 cm long, 2.5 mm diameter, Rhizosphere Research products, Wageningen, Netherlands). Pore-water samples were then gently transferred to 7.5 ml vials until overflow, and capped with 10 mm butyl rubber stoppers (Apodan Nordic, Denmark) with an aluminum crimp seal (Bastviken et al., 2010).

Back to the laboratory, 5 ml of pore-water samples were withdrawn from the vials by a glass syringe. Then, an air space was created in the syringe by adding 5 ml of pure nitrogen (Calgaz, Air Liquide, USA). The syringe was then vigorously agitated to equilibrate the gases between the two phases, and, after one minute, 1 ml of the air space sample was injected into a G2131-*i* CRDS analyzer operating in continuous flow mode with pure nitrogen (Calgaz, Air Liquide, USA) as carrier gas. Peak areas were then integrated and reported to a standard calibration curve created with pure nitrogen as a zero for both CO_2 and CH_4, and gas standard of 503 ppm for CO_2, and 100 ppm for CH_4 (Calgaz, Air Liquide, USA). All pore-water analyses were conducted within 4 h after sampling. All calculations were made following Bastviken et al. (Bastviken et al., 2010; Bastviken et al., 2008; Bastviken et al., 2004).

2.6. Physicochemical characteristics of the sedimentary column

Additional triplicate cores were collected twice for physicochemical analyses. A first collection was realized during the warm season, in January 2017, and a second was made during the cool season, in June 2017. Cores were then separated in six subsections of 10 cm. Redox potentials were measured using a combined Pt-Ag/Ag-Cl (reference) electrode connected to a WTW pH/mV/T meter. Redox data are reported relative to a standard hydrogen electrode, *i.e.*, after adding 202 mV to the original values obtained with an Ag/AgCl reference electrode at 25 °C (Marchand et al., 2011). pH was measured using a glass electrode and a WTW pH meter. The pH electrode was calibrated prior utilization using three standards solutions of pH 4, 7 and 9 at 25 °C (National Institute of Standards and Technology, USA). Pore-water salinity was measured using an Atago hand refractometer.

Total organic carbon (TOC) content and $\delta^{13}C$ were determined for each sampling period. TOC was analysed using a Total Organic Carbon Analyzer equipped with a SSM-5000A Solid Sample Module (TOC-LCPH-SSM500A, Shimadzu Corporation, Japan). $\delta^{13}C$ was measured using an elemental analyzer coupled to an isotope ratio mass spectrometer (Integra2, Sercon, UK). $\delta^{13}C$ values are reported in per mill (‰) deviations from a Pee Dee Belemnite (PDB) limestone carbonate for reference. Analytical precisions were check using IAEA-600 caffeine standard (IAEA Nucleus) and were <1% for TOC, and 0.3% for $\delta^{13}C$. All analyses were performed at the French Institute for the Sustainable Development (IRD) of Noumea, New Caledonia. Additional samples of roots, leaves, and surface sediment, the latest used as a proxy for biofilm isotopic value, were also analysed for $\delta^{13}C$.

2.7. Air temperature and chlorophyll-a

Air temperature was recorded before each measurement by a handheld thermometer. The relationships between CO_2 and CH_4 fluxes and temperature were estimated on an exponential basis (Lloyd and Taylor, 1994), and then, Q_{10} ratios, which represent the factor to be multiplied to the fluxes for a 10 °C rise, were calculated using the equation described by Xu and Qi (2001) and Chanda et al. (2013).

Soil surface chlorophyll-*a* (chl-*a*) was analysed for each measurement location. Samples for chlorophyll-*a* were firstly freeze-dried, and then a subsample of ~200 mg was weighted for extraction. Chl-*a* was extracted in the dark, at ambient temperature, in 8 ml of 93% methanol during 30 min. Concentrations were then determined using a fluorimeter (Yentsch and Menzel, 1963).

2.8. Statistical analyses

Student's *t*-tests were used to test the significant differences ($p < 0.05$) between seasons and between soil physicochemical parameters. The differences in seasonal, and light/dark CO_2 and CH_4 emissions, as well as the differences in soil $\delta^{13}C\text{-}CO_2$ values in light, dark, and dark after biofilm removal were tested using a two-way analysis of variance (ANOVA), followed by a Scheffe post-hoc test. The relationship between dark and light fluxes and the different parameters, were determined by simple linear regression analyses. All statistical analyses were performed under R software version 3.3.1 (R Development Core Team, 2008).

3. Results

3.1. Soil physicochemical characteristics

No significant variations with seasons of the physicochemical parameters studied were observed (two-sample t-tests, $p > 0.05$) (Fig. 1). TOC decreased from 22.23 ± 2.29% at the surface to 19.11 ± 0.61% at 25 cm depth, and then, increased with depth until 21.43 ± 1.29% at 55 cm depth, with a mean value 20.93 ± 2.14% (Fig. 1a).

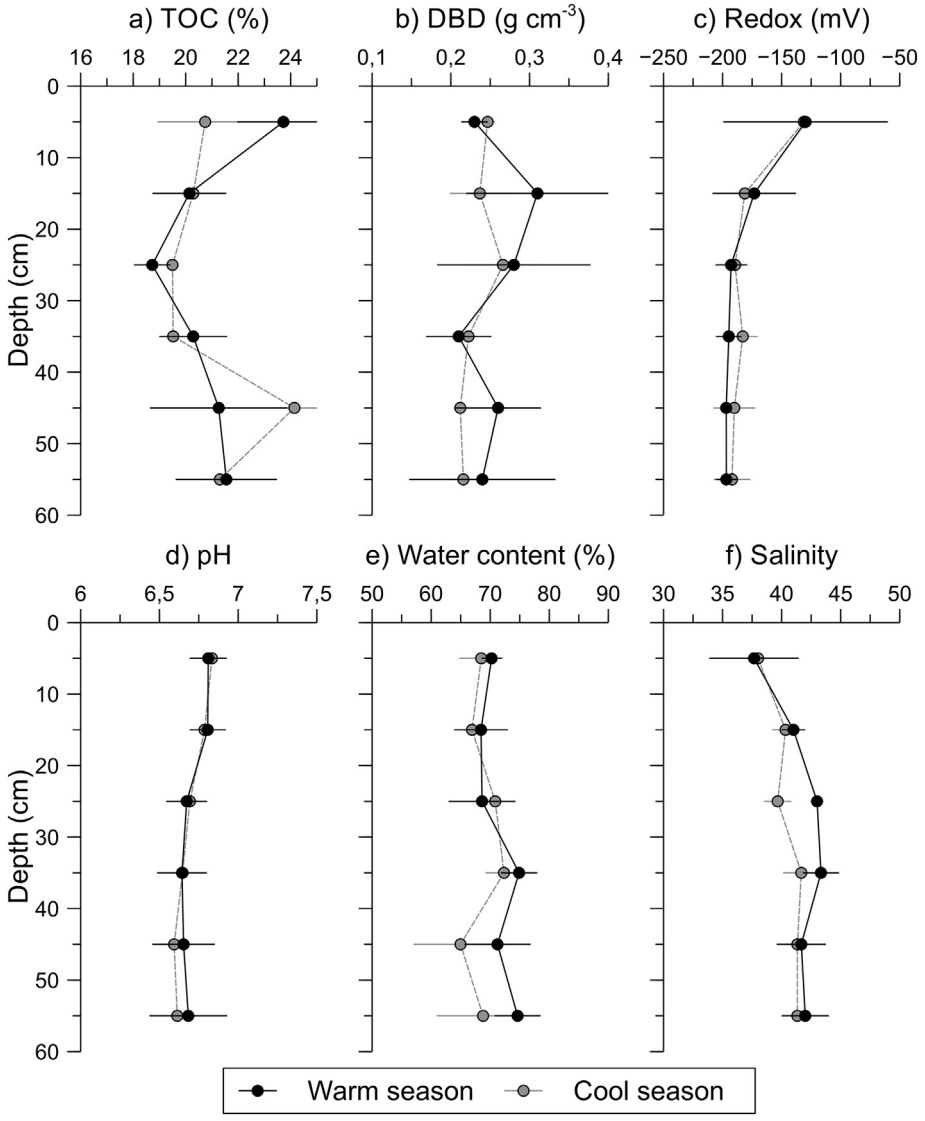

Fig. 1. Physicochemical profiles measured during the warm season (black lines) and the cool season (grey dotted lines). Each point is the mean of three replicates ± SD.

Mean value of dry bulk density (DBD) was 0.25 ± 0.06 g cm^{-3} (Fig. 1b). Redox potentials rapidly decreased from −130.43 ± 47.02 mV at the surface to −191.12 ± 10.99 mV at 15 cm depth, and then remained stable to the bottom of the core (Fig. 1c). pH and soil water content were almost invariable along the core profile, with mean values of 6.70 ± 0.14 and 70.29 ± 4.64%, respectively (Fig. 1d and e). Soil salinity increased from 37.83 ± 2.64 at the surface to 41.33 ± 1.97 at 15 cm depth, and remained stable until 55 cm depth (Fig. 1f).

3.2. CO_2 and CH_4 emissions

Considering the whole studied period, CO_2 and CH_4 emissions in light and in the dark ranged from 31.34 to 187.48 mmol m^{-2} day^{-1} and from 39.36 to 428.09 μmol m^{-2} day^{-1}, respectively (Fig. 2). Seasons had significant effects on both dark and light CO_2 and CH_4 fluxes (Table 1), which were higher during the warm season (Table 2). Significant differences were also observed between dark and light CO_2 fluxes (Table 1), either for the warm and the cool season, with higher emissions in the dark. In addition, CO_2 emissions in the dark, after having removed the upper 1–2 mm of soil, ranged from 145.22 to 282.30 mmol m^{-2} day^{-1} (Fig. 2), which was significantly higher than on intact soil surface (ranging from 57.64 to 187.48 mmol m^{-2} day^{-1}; two-sample *t*-test, $t_{(-5.31)} = 59.99$, $p < 0.001$). Moreover, CO_2 and CH_4 fluxes, measured in the dark, were positively correlated to fluxes measured at light (Fig. 3a and b; Table 3 Eqs. 1 and 2).

3.3. Relationships between CO_2 and CH_4 fluxes and temperature, soil gas concentrations and chlorophyll-a

Dark CO_2 and CH_4 fluxes were correlated to temperature in positive relationships (Fig. 4a and b; Table 3 Eqs. 5 and 6). Dark emissions without the upper 1–2 mm of soil were correlated to the dark emissions before removal (Fig. 4c and d; Table 3 Eqs. 3 and 4). In addition, positive correlations were also determined between dark and light CO_2 (Fig. 4c; Table 3 Eqs. 7 and 8) and CH_4 (Fig. 4d; Table 3 Eqs. 9 and 10) emissions and their respective soil concentrations. The slopes of these two last relationships were higher for dark incubation compared to light ones. Eventually, the difference between dark and light fluxes was related to the soil surface chlorophyll-*a* concentrations (Fig. 5; Table 3 Eq. 11).

3.4. $\delta^{13}C$ and $\delta^{13}C$-CO_2

Mean $\delta^{13}C$-CO_2 values of the CO_2-emitted during soil incubations at light, in the dark and in the dark after having removed the upper

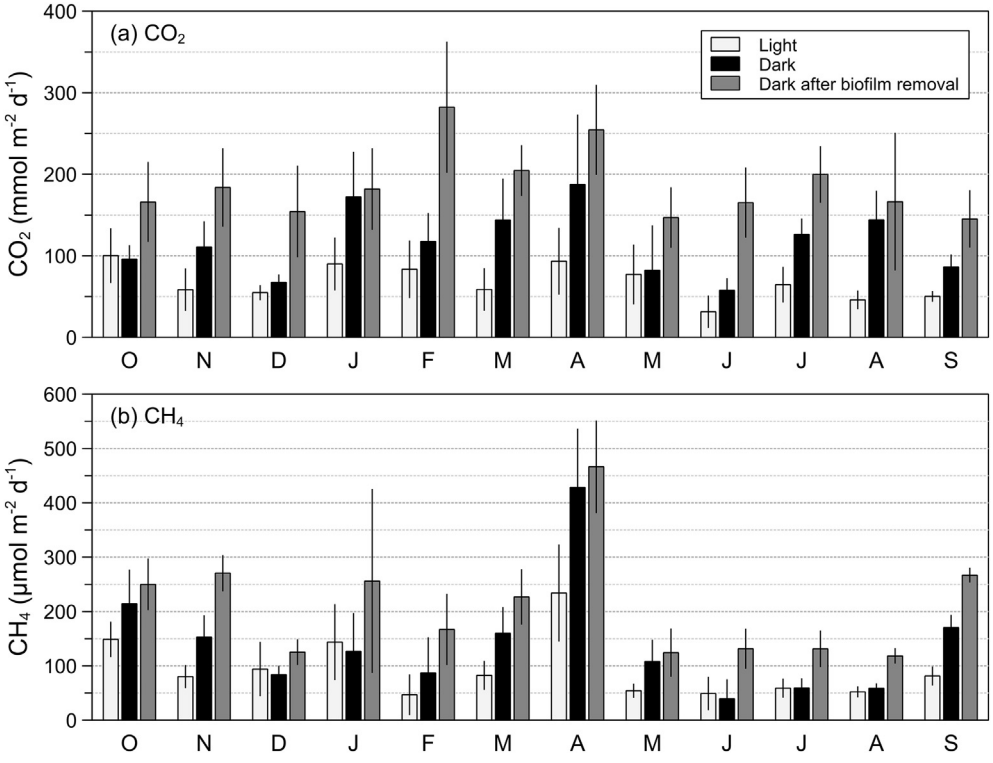

Fig. 2. (a) CO_2 (mmol m^{-2} day^{-1}) and (b) CH_4 (µmol m^{-2} day^{-1}) fluxes in light, in the dark, and in the dark after removing the biofilm, during the studied period, from October 2016 to September 2017. Means of 9 replicates ± SD.

1–2 mm of soil were − 19.75 ± 2.88‰, −20.17 ± 2.38‰ and − 15.92 ± 2.44‰, respectively. Consequently, dark δ^{13}C-CO_2 values were thus the more depleted, however the difference between light and dark fluxes were not significant ($p > 0.05$). In addition, the difference of dark and light δ^{13}C-CO_2 values was correlated to the difference of dark and light CO_2 fluxes in a negative relation (Fig. 6; Table 3 Eq. 12). Furthermore, the δ^{13}C-CO_2 value of the CO_2 emitted in the dark after removal of the upper 1–2 mm of soil was significantly higher than at light and in the dark (two-way ANOVA, $F_{(1,278)} = 75.51$; $p < 0.001$).

The δ^{13}C values of roots, leaves, soil surface and soil column, as well as the δ^{13}C-CO_2 signatures of the CO_2-emitted by root respiration and leaf litter decomposition are presented in Table 4.

4. Discussion

4.1. Mangrove soils as a net source of CO_2 and CH_4 to the atmosphere

Soil CO_2 and CH_4 emissions to the atmosphere in the studied mangrove forest were elevated throughout the year. Mean CO_2 emissions ranged from 31.35 to 282.30 mmol m^{-2} day^{-1} (Fig. 2), and therefore confirmed those measured previously in another *Rhizophora* mangrove forest in New Caledonia by Leopold et al. (2013 and 2015), for which CO_2 fluxes ranged from 14.5 to 262.8 mmol m^{-2} day^{-1}. Furthermore, in a broader study of eleven mangrove swamps in the Caribbean, in Australia and in New Zealand, Lovelock (2008) evaluated the soil CO_2 fluxes to range from −21.6 to 256.6 mmol m^{-2} day^{-1}. Later, Bulmer et al. (2015) measured mean CO_2 emissions of 168.5 ± 45.8 mmol m^{-2} day^{-1} in a mangrove developing at higher latitudes (New Zealand). Only mangroves subjected to strong eutrophication were reported to have high CO_2 emissions, and for example up to 749.34 mmol m^{-2} day^{-1} in Hong Kong (Chen et al., 2012). Eventually, CO_2 fluxes measured in the present study were higher than the compilation from 140 study sites made by Alongi (2014), who reported mean CO_2 emissions of 69 ± 8 mmol m^{-2} day^{-1}. Regarding CH_4, fluxes measured in the present study ranged from 39.36 to 466.33 µmol m^{-2} day^{-1} (Fig. 2). When converted into CO_2-equivalent, considering its 100-year global warming potential (Myhre et al., 2013), CH_4 represented 1% of the total emissions measured (CO_2 + CH_4). CH_4 emissions were in the same range as those measured in previous studies, as for instance in the Sundarbans, where CH_4 fluxes ranged from 1.97 to 567.12 µmol m^{-2} day^{-1} (Biswas et al., 2007; Chanda et al., 2013), or in Australia, where CH_4 fluxes ranged from 30 to 520 µmol m^{-2} day^{-1} (Kreuzwieser et al., 2003). Eventually, CH_4 emissions were also in the same range as those reported by (Chen et al., 2014) in Indonesia (−145.2 to 315.36 µmol m^{-2} day^{-1}). In addition, the CO_2 and CO_4 emissions recorded at low tide in this study were much more higher, >27 for CO_2 and 6 for CH_4, than those measured in the same location during high tide (Jacotot et al., 2018), which were 3.35 mmol m^{-2} day^{-1} and 18.30 µmol m^{-2} day^{-1} for CO_2 and CH_4, respectively. Higher emissions during low tide may be explained by

Table 1
F values of two-way ANOVA tests showing the seasonal and dark/light effects on CO_2 and CH_4 emissions.

Parameters	Sources of variation		
	Season	Dark/Light	Interaction
CO_2	13.833***	56.848***	0.187^{NS}
CH_4	26.715***	15.422***	3.423^{NS}

NS: non-significant.
*** Indicates significant effects at $p < 0.001$.

Table 2
Mean seasonal emissions ($n = 54 \pm$ SD measures per season) of CO_2 (mmol m^{-2} day^{-1}) and CH_4 (µmol m^{-2} day^{-1}), in the light and in the dark.

Parameters	Dark		Light	
Season	Warm	Cool	Warm	Cool
CO_2	126.97 (59.12)^{a}	98.96 (44.22)^{b}	77.16 (33.09)^{bc}	54.79 (28.57)^{c}
CH_4	146.30 (115.80)^{a}	69.79 (37.78)^{b}	97.41 (75.43)^{bc}	54.12 (17.02)^{c}

Different letters indicate significant differences (Scheffe post-hoc test, $p < 0.05$).

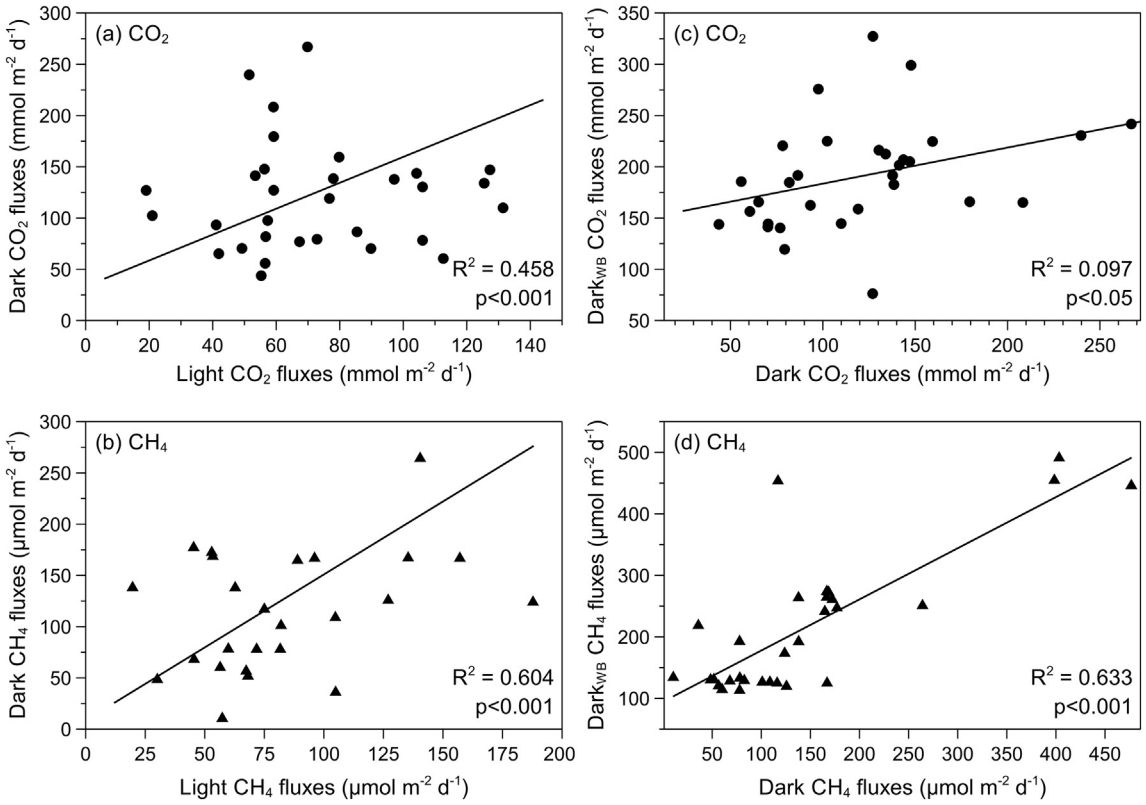

Fig. 3. (a) and (b): Relationship between light and dark fluxes of CO_2 (mmol m^{-2} day^{-1}) and CH_4 (µmol m^{-2} day^{-1}); (c) and (d): Relationship between dark fluxes without the upper 1–2 mm of soil ($Dark_{WB}$) and dark fluxes of CO_2 (mmol m^{-2} day^{-1}) and CH_4 (µmol m^{-2} day^{-1}); $n = 36$, each point is the mean of three replicates.

oxygen diffusion within the soil, which enhanced organic matter decomposition, and by the easier gases diffusion in the atmosphere than in water.

However, when compared to other ecosystems, CO_2 and CH_4 emissions from the studied mangrove soil were much lower (Oertel et al., 2016). For example, CO_2 emissions in the present study were twice lower than the CO_2 emissions in some tropical rainforests from Malaysia, Hawaii and Brazil, which were evaluated to range from 295.7 to 598.4 mmol m^{-2} day^{-1} (Katayama et al., 2009; Litton et al., 2011; Metcalfe et al., 2007). Similar observations can be made regarding CH_4, which may be emitted in very large quantities from interior tropical wetlands (Sjögersten et al., 2014). Therefore, even if mangroves are among the carbon-richest forests in the world (Donato et al., 2011), they emit low quantities of greenhouse gas. This particularity mainly derives from the waterlogging conditions of their soils, which favor anaerobic organic matter decomposition, which is less efficient than aerobic decay processes. However, even if CO_2 and CH_4 emissions from mangrove soils are low, they are highly variable, and depend notably on season, or on the development of biofilm at the soil surface, which may sometimes induce negative fluxes (*e.g.* Chen et al., 2014; Bulmer et al., 2015; Wang et al., 2016).

4.2. Seasonal variability of CO_2 and CH_4 emissions

Seasonal differences in CO_2 and CH_4 emissions were evidenced in the present study, with higher values during the warm season (Table 2). Several environmental factors may influence GHG emissions to the atmosphere, including notably the physicochemical properties of the soil and its water content (Bulmer et al., 2015; Chanda et al., 2013; Kirui et al., 2009; Leopold et al., 2015, 2013; Livesley and Andrusiak, 2012; Poungparn et al., 2009). Herein, fluxes measurements were performed between 2 h prior and after the low tide, when the soil was the most unsaturated in water. Consequently, we are confident that variations in soil water content due to the tidal cycle were not involved in the variability of the fluxes. In addition, no significant variations between the two seasons were observed for the physicochemical

Table 3
List of the different equations of regression, the R^2 (coefficient of determination) and the corresponding *p*-values.

Equations of regression		R^2	p-values	Figures
Dark CO_2 fluxes = 33.3227 * Light CO_2 fluxes + 1.2632	(1)	0.458	<0.001	Fig. 3a
Dark CH_4 fluxes = 8.5342 * Light CH_4 fluxes + 1.4237	(2)	0.604	<0.001	Fig. 3b
$Dark_{WB}$ CO_2 fluxes = 148.3216 * Dark CO_2 fluxes + 0.3521	(3)	0.097	<0.05	Fig. 3c
$Dark_{WB}$ CH_4 fluxes = 94.6615 * Dark CH_4 fluxes + 0.8317	(4)	0.633	<0.001	Fig. 3d
Dark CO_2 fluxes = 17.85113 * exp^(0.08698 * Temperature)	(5)	0.366	<0.05	Fig. 4a
Dark CH_4 fluxes = 0.5 * exp^(0.2029 * Temperature)	(6)	0.244	<0.05	Fig. 4b
Dark CO_2 fluxes = 158.494 * soil CO_2 concentrations + 9.105	(7)	0.763	<0.01	Fig. 4c
Light CO_2 fluxes = 58.9 * soil CO_2 concentrations + 24.63	(8)	0.441	<0.05	Fig. 4c
Dark CH_4 fluxes = 358.27 * soil CH_4 concentrations − 151.29	(9)	0.952	<0.001	Fig. 4d
Light CH_4 fluxes = 171.38 * soil CH_4 concentrations − 42.95	(10)	0.768	<0.01	Fig. 4d
Dark-light CO_2 fluxes = 1.258 * soil chl-a − 12.828	(11)	0.323	<0.05	Fig. 5
Dark-Light fluxes = 61.222 * Dark-Light δ^{13}C-CO_2 − 11.819	(12)	0.291	<0.01	Fig. 6

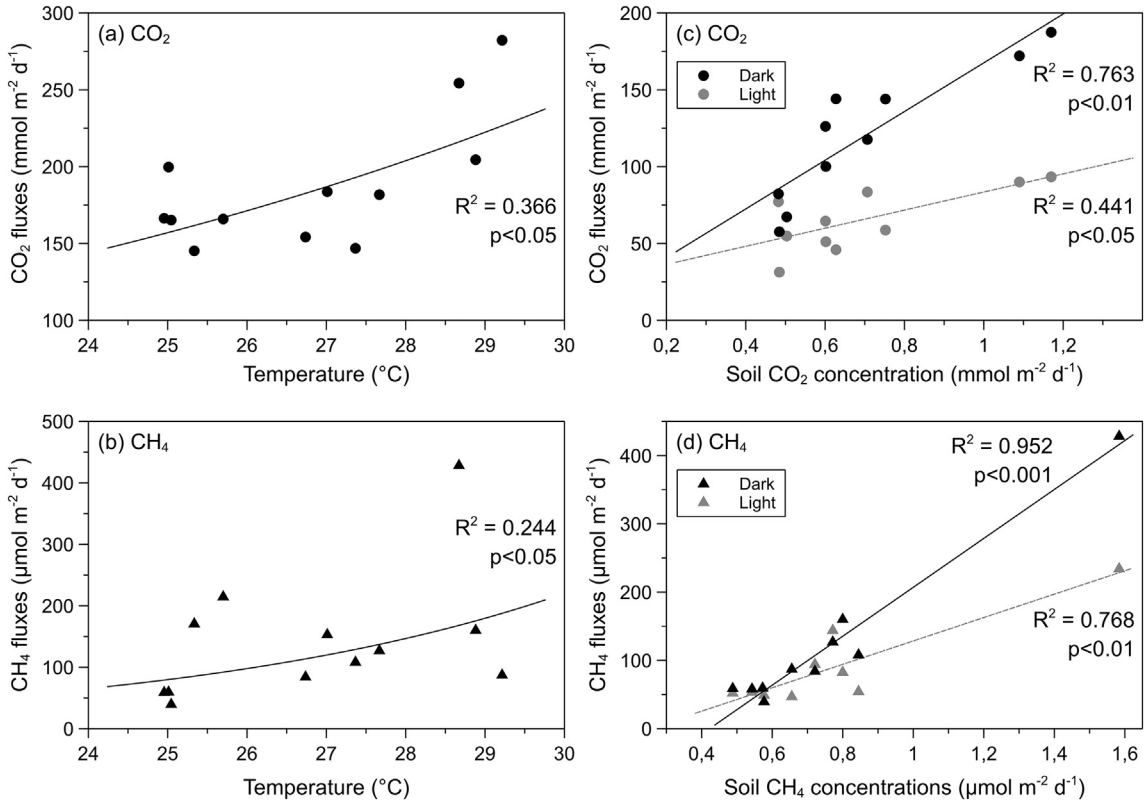

Fig. 4. (a) and (b): Relationship between CO_2 (mmol m^{-2} day^{-1}) and CH_4 (µmol m^{-2} day^{-1}) fluxes and temperature (°C); $n = 12$, each point is the mean of 9 replicates. (c) and (d): Relationship between CO_2 (mmol m^{-2} day^{-1}) and CH_4 (µmol m^{-2} day^{-1}) fluxes and soil CO_2 (mmol m^{-2} day^{-1}) and CH_4 (µmol m^{-2} day^{-1}) concentrations, in the dark (dark points) and at light (grey points); $n = 10$; each point is the mean of 3 replicates.

parameters (Fig. 1), suggesting that these parameters were not involved in the seasonal difference of CO_2 and CH_4 fluxes. This absence of variability in the physicochemical parameters studied may be surprising but is suggested to result from the position of the study site, in the lowest intertidal zone, in which tides are coming twice a day, possibly buffering redox, pH and salinity variations.

Higher CO_2 fluxes to the atmosphere with warmer temperatures was consistent with other studies in terrestrial ecosystems (Lou et al., 2003; Parkin and Kaspar, 2003; Raich and Schlesinger, 1992), including mangroves (Allen et al., 2011; Chen et al., 2012; Leopold et al., 2015). Similarly, several studies showed that temperature is a major factor driving CH_4 emissions to the atmosphere in terrestrial wetlands (Bubier et al., 1995; Crill et al., 1988; Moore and Knowles, 1990; Trudeau et al., 2013; Turetsky et al., 2008) or in tidal wetlands (Sun et al., 2013; Wang et al., 2015). Estimated Q_{10} value for CO_2 emissions in the studied mangrove was 2.39, which was in complete accordance with other values reported for mangrove ecosystems (Leopold et al., 2015; Lovelock, 2008) or even for terrestrial ecosystems (Raich and Schlesinger, 1992). Concerning CH_4, Q_{10} value in this study was 7.61, and thus was higher than for CO_2, suggesting that CH_4 production was more sensitive to temperature variations. Q_{10} values of methane production in oligotrophic wetlands environments, such as mangroves, are described as having a wide range of variation, from 1.7 to 28 (Segers, 1998), which is thus consistent with our findings. The

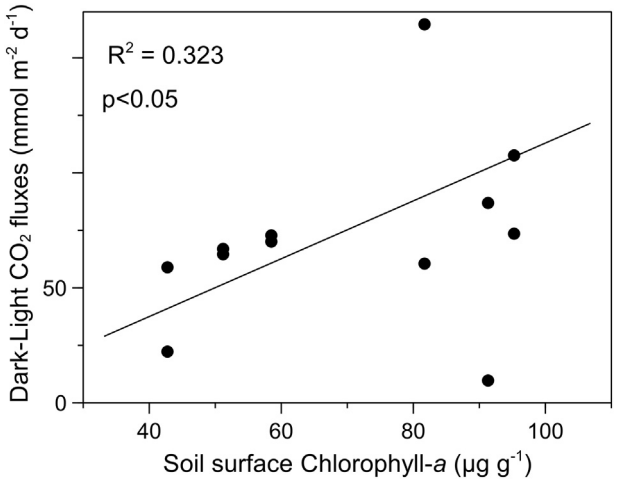

Fig. 5. Relationship between the difference in Dark and Light CO_2 fluxes (mmol m^{-2} day^{-1}) and chlorophyll-*a* soil surface concentration (µg g^{-1}). $n = 12$, each point is the mean of three replicates.

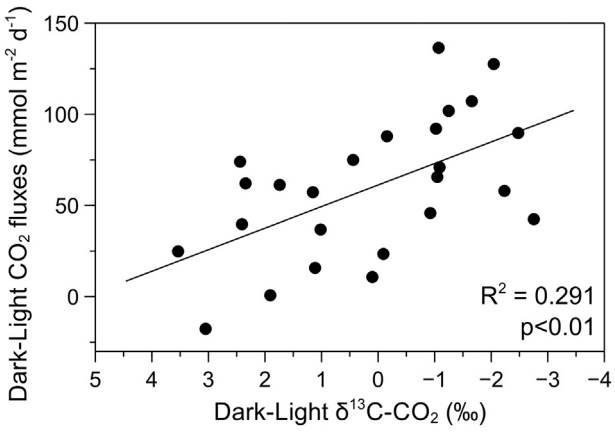

Fig. 6. Difference in dark and light fluxes (mmol m^{-2} day^{-1}) as a function of the difference between dark and light $\delta^{13}C$-CO_2 (‰). $n = 25$, each point representing the mean of three replicates.

Table 4
$\delta^{13}C$ (‰ (SD)) values for roots, leaves, soil surface (1–2 mm depth) and for the soil column (0–50 cm depth, $n = 6$); and $\delta^{13}C\text{-}CO_2$ (‰ (SD)) emitted by roots respiration ($n = 3$) and leaf litter decomposition ($n = 3$).

Parameters	Roots	Leaf litter	Soil surface (1-2 mm)	Soil column (0–60 cm)
$\delta^{13}C$ (‰)	−25.88	−23.86	−18.67	−22.33 (1.82)
$\delta^{13}C\text{-}CO_2$ (‰)	−22.32 (1.06)	−21.43 (1.89)	*Na*	*Na*

Na: Non-available.

temperature sensitivity of biogeochemical processes, such as soil organic matter decomposition by respiration and methanogenesis, have been widely described in the literature for different ecosystems (Conant et al., 2011; Davidson and Janssens, 2006; Fang and Moncrieff, 2001; Fierer et al., 2005; Inglett et al., 2012; Segers, 1998), including mangroves (Barroso-Matos et al., 2012; Mackey and Smail, 1996). Consequently, soil gases production, and thus, their emissions at the soil-air interface, may increase with temperature. In fact, higher average soil CO_2 and CH_4 concentrations were measured in this study during the warm season in comparison to the cool season, therefore adding to the hypothesis of a temperature control on soil greenhouse gas production.

In addition, strong relationships were found between soil CO_2 and CH_4 concentrations and their respective emissions at the soil-air interface (Fig. 4c and d), therefore confirming that soil greenhouse gas concentrations are another primary factor in greenhouse gas emissions to the atmosphere. However, our result showed that for the same soil gas concentrations, fluxes were lower when measurements where performed at light (Fig. 4c and d), suggesting that other constraining factors were involved during light incubations, like, possibly, biofilm, as demonstrated in other studies (*e.g.* Bulmer et al., 2015; Leopold et al., 2013, 2015).

4.3. Evidences of biofilm control on CO_2 and CH_4 emissions

CO_2 emitted at the surface of mangrove soils derives from various sources such as: roots respiration, leaf litter decomposition, organic-matter degradation, as well as biofilm respiration and degradation. The $\delta^{13}C\text{-}CO_2$ value of the emitted CO_2 is therefore a mixture of the specific values of the CO_2 produced by these different sources. In the present study, the $\delta^{13}C\text{-}CO_2$ value of the CO_2 emitted by roots respiration was -22.32 ± 1.06‰, while it was -21.43 ± 1.89‰ for leaf litter decomposition (Table 4). Although the isotopic value of the CO_2 produced by organic matter decomposition within the soil was not measured in this study, some authors reported low fractionation during organic matter decomposition, and, consequently, a low difference between the $\delta^{13}C$ value of the source and the $\delta^{13}C\text{-}CO_2$ value of the produced CO_2 (Lin and Ehleringer, 1997; Maher et al., 2015). Therefore, we used the mean $\delta^{13}C$ value of the organic matter in the soil, -22.33 ± 1.82‰, as a proxy of the $\delta^{13}C$ value of the CO_2 produced by its decomposition. Consequently, these three sources all had $\delta^{13}C\text{-}CO_2$ values lower than −21.43‰, whereas the mean $\delta^{13}C$ value of the CO_2 emitted at the soil-air interface was -19.76 ± 1.19‰, therefore suggesting that another source must be involved in the emissions. Biofilm is mainly composed by an assemblage of heterotrophic bacteria and autotrophic eukaryotes (Bouchez et al., 2013; Decho, 2000) that are $\delta^{13}C$ enriched comparatively to mangrove organic matter (Bouillon et al., 2002; Coffin et al., 1989; Khan et al., 2015; Lamb et al., 2006). We, thus, suggest that the $\delta^{13}C$ value of the CO_2 fluxes demonstrated that biofilm respiration/photosynthesis and/or its decomposition contributed to CO_2 and CH_4 emissions along with the roots respiration, and soil organic matter decomposition.

Apart from few measurements, CO_2 emissions at the soil surface were always higher in the dark than at light. This result suggests that, at light, CO_2 diffusing from mangrove soils may be consumed by the primary producers composing the biofilm during photosynthesis processes, as suggested in previous studies (Bulmer et al., 2015; Chen et al., 2014; Wang et al., 2016). This process was also evidenced by a positive relationship between the difference in dark and light CO_2 fluxes and the soil surface chlorophyll-*a* (Fig. 6). More biofilm implies more consumption of the CO_2 during photosynthesis, and therefore higher difference between dark and light fluxes. In addition, due to carbon fractionation during photosynthesis, which uses ^{12}C preferentially to ^{13}C (Farquhar et al., 1989; O'Leary, 1988), the $\delta^{13}C\text{-}CO_2$ measured during light incubations should have an enriched value, relatively to the one measured during dark incubations. Consequently, as the rate of photosynthesis increases, the difference between dark $\delta^{13}C\text{-}CO_2$ and light $\delta^{13}C\text{-}CO_2$ may decrease. Such a variation was observed in this study (Fig. 6), therefore confirming that photosynthetic activity was involved in the reduction of the CO_2 emissions at the soil surface.

Higher CH_4 fluxes were also observed during dark incubations relatively to light incubations (Fig. 3b). Similarly to CO_2, biofilm may act as a sink for CH_4, since anaerobic oxidation of methane by anaerobic methanotrophic archaea and sulphate-reducing bacteria may occur (Cui et al., 2015). However, the absence of correlation between dark and light emissions and the soil surface chlorophyll-*a* tends to indicate that biofilm was not involved in the reduction of CH_4 emissions at light. We suggest that the lower emissions at light may result from CH_4 photo-oxidation processes, as evidenced in others studies (Dutta et al., 2017; Johnston and Kinnison, 1998). Consequently, strong differences between light and dark CO_2 and CH_4 fluxes were measured. Considering that mangroves are subject to the daily cycle of light, we suggest that these differences should be taken into account in future carbon budgets, since light and dark fluxes each account for only half of the daily emissions.

Previous studies suggested another role of the microphytobenthos in GHG emissions, reducing them by forming a physical barrier at the soil surface (Bulmer et al., 2015; Leopold et al., 2015, 2013). In our study, removing the upper 1–2 mm of soil also lead to an enhancement of the CO_2 emissions that were multiplied by a factor of 1.75, which is consistent with the 2.2 factor reported by (Leopold et al., 2015) in another *Rhizophora* mangrove forest in New Caledonia. However, after removal, significant enriched values of $\delta^{13}C\text{-}CO_2$ (mean of -16.70 ± 2.70‰) were measured compared to the ones obtained before removal (mean of -19.76 ± 1.19‰). Such a result was surprising as we expected a greater contribution of the CO_2 produced within the soil, characterized by $\delta^{13}C$ values lower than −21.59‰. Consequently, we suggest that removing the upper 1–2 mm of soil resulted in a partial removal of the biofilm but also and mainly to its deterioration, inducing higher CO_2 emissions and depleted $\delta^{13}C\text{-}CO_2$ values. However, the strong positive relationship between dark CH_4 emissions before and after biofilm removal supports the hypothesis that the biofilm acts as a physical barrier preventing GHG emissions (Fig. 3d). Methanogenesis is a strictly anaerobic process that only occurs in the deep anoxic sediment layers (Dutta et al., 2015; Dutta et al., 2013), and is suggested not to be enhanced by biofilm removal. Similar relationship was also observed for CO_2 (Fig. 3c), therefore adding to the previous finding, however, the relationship was weaker than for CH_4, suggesting that both biodegradation and absence of physical barriers properties were involved in the higher CO_2 emissions after the removal of the upper 1–2 mm of soil.

5. Conclusions

CO_2 and CH_4 emissions from a *Rhizophora* mangrove soil were relatively low throughout the year, with CH_4 representing only 1% of the combined CO_2 and CH_4 emissions. Nevertheless, GHG fluxes showed a high seasonal variability, with higher values measured during the warm season. We suggest that these enhanced emissions mainly derived from increased organic matter decomposition rates due to elevated temperature, higher CO_2 and CH_4 concentrations were measured within the soil. In addition, CO_2 and CH_4 emissions were

controlled by biofilm development at the soil surface. First, biofilm may act as a physical barrier preventing the gases to reach the atmosphere. In addition, by measuring δ^{13}C-CO_2 values of the CO_2 emitted in the dark and at light, we were able to confirm the reduction of CO_2 emissions by its consumption during photosynthesis processes at sediment surface. However, we were not able to evaluate the respective contribution of each CO_2 source within the soil due to their too close δ^{13}C-CO_2 values. Eventually, we observed that removing the upper 1–2 mm of soil resulted only in a partial removal of the biofilm but also and mainly to its deterioration, inducing higher CO_2 emissions and depleted δ^{13}C-CO_2 values.

Although some forcing factors remain unidentified, major advances have been made during the last few years in the evaluation of the greenhouse gas emissions from mangrove soils. However, all the studies focused on fluxes during emersion periods, consequently occulting inundation periods. Due to their position, mangroves are regularly flooded, and up to half of the time for some regions, which may severely contribute to the emissions of greenhouse gas. Consequently, we suggest that further studies may focus on these potential emissions.

Acknowledgments

This work was funded by the Province Sud of New Caledonia, the City of Mont Dore, KNS Koniambo Nickel SAS, Vale NC, and the GOPS. The authors thank the Air Liquide Foundation for funding the CRDS analyzer. The authors are grateful to Inès Gayral for her support in field work.

Declaration of interest

Authors have no conflict of interest to declare.

References

Allen, D.E., Dalal, R.C., Rennenberg, H., Meyer, R.L., Reeves, S., Schmidt, S., 2007. Spatial and temporal variation of nitrous oxide and methane flux between subtropical mangrove sediments and the atmosphere. Soil Biol. Biochem. 39, 622–631. https://doi.org/10.1016/j.soilbio.2006.09.013.

Allen, D., Dalal, R.C., Rennenberg, H., Schmidt, S., 2011. Seasonal variation in nitrous oxide and methane emissions from subtropical estuary and coastal mangrove sediments, Australia. Plant Biol. 13, 126–133.

Alongi, D.M., 2014. Carbon cycling and storage in mangrove forests. Annu. Rev. Mar. Sci. 6, 195–219. https://doi.org/10.1146/annurev-marine-010213-135020.

Alongi, D.M., Wattayakorn, G., Pfitzner, J., Tirendi, F., Zagorskis, I., Brunskill, G.J., Davidson, A., Clough, B.F., 2001. Organic carbon accumulation and metabolic pathways in sediments of mangrove forests in southern Thailand. Mar. Geol. 179, 85–103. https://doi.org/10.1016/S0025-3227(01)00195-5.

Alongi, D.M., Sasekumar, A., Chong, V.C., Pfitzner, J., Trott, L.A., Tirendi, F., Dixon, P., Brunskill, G.J., 2004. Sediment accumulation and organic material flux in a managed mangrove ecosystem: estimates of land–ocean–atmosphere exchange in peninsular Malaysia. Mar. Geol. 208, 383–402. https://doi.org/10.1016/j.margeo.2004.04.016 Material Exchange Between the Upper Continental Shelf and Mangrove Fringed Coasts with Special Reference to the N. Amazon-Guianas Coast.

Barbier, E.B., Hacker, S.D., Kennedy, C., Koch, E.W., Stier, A.C., Silliman, B.R., 2011. The value of estuarine and coastal ecosystem services. Ecol. Monogr. 81, 169–193. https://doi.org/10.1890/10-1510.1.

Barroso-Matos, T., Bernini, E., Eduardo Rezende, C., 2012. Decomposition of mangrove leaves in the estuary of Paraíba do Sul RiverRio de Janeiro, Brazil. Lat. Am. J. Aquat. Res. 40, 398–407.

Bastviken, D., Cole, J., Pace, M., Tranvik, L., 2004. Methane emissions from lakes: dependence of lake characteristics, two regional assessments, and a global estimate: lake methane emissions. Glob. Biogeochem. Cycles 18. https://doi.org/10.1029/2004GB002238 n/a-n/a.

Bastviken, D., Cole, J.J., Pace, M.L., Van de Bogert, M.C., 2008. Fates of methane from different lake habitats: Connecting whole-lake budgets and CH 4 emissions: Fates of lake methane. J. Geophys. Res. Biogeosci. 113. https://doi.org/10.1029/2007JG000608 n/a-n/a.

Bastviken, D., Santoro, A.L., Marotta, H., Pinho, L.Q., Calheiros, D.F., Crill, P., Enrich-Prast, A., 2010. Methane emissions from Pantanal, South America, during the low water season: toward more comprehensive sampling. Environ. Sci. Technol. 44, 5450–5455. https://doi.org/10.1021/es1005048.

Biswas, H., Mukhopadhyay, S.K., Sen, S., Jana, T.K., 2007. Spatial and temporal patterns of methane dynamics in the tropical mangrove dominated estuary, NE coast of bay of Bengal, India. J. Mar. Syst. 68, 55–64. https://doi.org/10.1016/j.jmarsys.2006.11.001.

Bouchez, A., Pascault, N., Chardon, C., Bouvy, M., Cecchi, P., Lambs, L., Herteman, M., Fromard, F., Got, P., Leboulanger, C., 2013. Mangrove microbial diversity and the impact of trophic contamination. Mar. Pollut. Bull. 66, 39–46. https://doi.org/10.1016/j.marpolbul.2012.11.015.

Bouillon, S., Koedam, N., Raman, A., Dehairs, F., 2002. Primary producers sustaining macro-invertebrate communities in intertidal mangrove forests. Oecologia 130, 441–448.

Bouillon, S., Borges, A.V., Castañeda-Moya, E., Diele, K., Dittmar, T., Duke, N.C., Kristensen, E., Lee, S.Y., Marchand, C., Middelburg, J.J., et al., 2008. Mangrove production and carbon sinks: a revision of global budget estimates. Glob. Biogeochem. Cycles 22.

Breithaupt, J.L., Smoak, J.M., Smith, T.J., Sanders, C.J., Hoare, A., 2012. Organic carbon burial rates in mangrove sediments: strengthening the global budget: mangrove organic carbon burial rates. Glob. Biogeochem. Cycles 26. https://doi.org/10.1029/2012GB004375.

Bubier, J.L., Moore, T.R., Bellisario, L., Comer, N.T., Crill, P.M., 1995. Ecological controls on methane emissions from a northern peatland complex in the zone of discontinuous permafrost, Manitoba, Canada. Glob. Biogeochem. Cycles 9, 455–470. https://doi.org/10.1029/95GB02379.

Bulmer, R.H., Lundquist, C.J., Schwendenmann, L., 2015. Sediment properties and CO_2 efflux from intact and cleared temperate mangrove forests. Biogeosciences 12, 6169–6180. https://doi.org/10.5194/bg-12-6169-2015.

Chanda, A., Akhand, A., Manna, S., Dutta, S., Das, I., Hazra, S., Rao, K.H., Dadhwal, V.K., 2013. Measuring daytime CO2 fluxes from the inter-tidal mangrove soils of Indian Sundarbans. Environ. Earth Sci. 72, 417–427. https://doi.org/10.1007/s12665-013-2962-2.

Chauhan, R., Datta, A., Ramanathan, A., Adhya, T.K., 2015. Factors influencing spatio-temporal variation of methane and nitrous oxide emission from a tropical mangrove of eastern coast of India. Atmos. Environ. 107, 95–106. https://doi.org/10.1016/j.atmosenv.2015.02.006.

Chen, G.C., Tam, N.F.Y., Ye, Y., 2012. Spatial and seasonal variations of atmospheric N2O and CO2 fluxes from a subtropical mangrove swamp and their relationships with soil characteristics. Soil Biol. Biochem. 48, 175–181. https://doi.org/10.1016/j.soilbio.2012.01.029.

Chen, G.C., Ulumuddin, Y.I., Pramudji, S., Chen, S.Y., Chen, B., Ye, Y., Ou, D.Y., Ma, Z.Y., Huang, H., Wang, J.K., 2014. Rich soil carbon and nitrogen but low atmospheric greenhouse gas fluxes from North Sulawesi mangrove swamps in Indonesia. Sci. Total Environ. 487, 91–96. https://doi.org/10.1016/j.scitotenv.2014.03.140.

Chen, G., Chen, B., Yu, D., Tam, N.F.Y., Ye, Y., Chen, S., 2016a. Soil greenhouse gas emissions reduce the contribution of mangrove plants to the atmospheric cooling effect. Environ. Res. Lett. 11, 124019. https://doi.org/10.1088/1748-9326/11/12/124019.

Chen, G., Chen, B., Yu, D., Ye, Y., Tam, N.F.Y., Chen, S., 2016b. Soil greenhouse gases emissions reduce the benefit of mangrove plant to mitigating atmospheric warming effect. Biogeosci. Discuss., 1–22 https://doi.org/10.5194/bg-2015-662.

Coffin, R.B., Fry, B., Peterson, B.J., Wright, R.T., 1989. Carbon isotopic compositions of estuarine bacteria. Limnol. Oceanogr. 34, 1305–1310.

Conant, R.T., Ryan, M.G., AAgren, G.I., Birge, H.E., Davidson, E.A., Eliasson, P.E., Evans, S.E., Frey, S.D., Giardina, C.P., Hopkins, F.M., 2011. Temperature and soil organic matter decomposition rates–synthesis of current knowledge and a way forward. Glob. Change Biol. 17, 3392–3404.

Crill, P.M., Bartlett, K.B., Harriss, R.C., Gorham, E., Verry, E.S., Sebacher, D.I., Madzar, L., Sanner, W., 1988. Methane flux from Minnesota peatlands. Glob. Biogeochem. Cycles 2, 371–384. https://doi.org/10.1029/GB002i004p00371.

Cui, M., Ma, A., Qi, H., Zhuang, X., Zhuang, G., 2015. Anaerobic oxidation of methane: an "active" microbial process. MicrobiologyOpen 4, 1–11.

Davidson, E.A., Janssens, I.A., 2006. Temperature sensitivity of soil carbon decomposition and feedbacks to climate change. Nature 440, 165–173. https://doi.org/10.1038/nature04514.

Decho, A.W., 2000. Microbial biofilms in intertidal systems: an overview. Cont. Shelf Res. 20, 1257–1273. https://doi.org/10.1016/S0278-4343(00)00022-4.

Donato, D.C., Kauffman, J.B., Murdiyarso, D., Kurnianto, S., Stidham, M., Kanninen, M., 2011. Mangroves among the most carbon-rich forests in the tropics. Nat. Geosci. 4, 293–297. https://doi.org/10.1038/ngeo1123.

Dutta, M.K., Chowdhury, C., Jana, T.K., Mukhopadhyay, S.K., 2013. Dynamics and exchange fluxes of methane in the estuarine mangrove environment of the Sundarbans, NE coast of India. Atmos. Environ. 77, 631–639. https://doi.org/10.1016/j.atmosenv.2013.05.050.

Dutta, M.K., Mukherjee, R., Jana, T.K., Mukhopadhyay, S.K., 2015. Biogeochemical dynamics of exogenous methane in an estuary associated to a mangrove biosphere; the Sundarbans, NE coast of India. Mar. Chem. 170, 1–10. https://doi.org/10.1016/j.marchem.2014.12.006.

Dutta, M.K., Bianchi, T.S., Mukhopadhyay, S.K., 2017. Mangrove methane biogeochemistry in the Indian Sundarbans: a proposed budget. Front. Mar. Sci. 4. https://doi.org/10.3389/fmars.2017.00187.

Fang, C., Moncrieff, J.B., 2001. The dependence of soil CO2 efflux on temperature. Soil Biol. Biochem. 33, 155–165. https://doi.org/10.1016/S0038-0717(00)00125-5.

Farquhar, G.D., Ehleringer, J.R., Hubick, K.T., 1989. Carbon isotope discrimination and photosynthesis. Annu. Rev. Plant Biol. 40, 503–537.

Fierer, N., Craine, J.M., McLauchlan, K., Schimel, J.P., 2005. Litter quality and the temperature sensitivity of decomposition. Ecology 86, 320–326. https://doi.org/10.1890/04-1254.

Inglett, K.S., Inglett, P.W., Reddy, K.R., Osborne, T.Z., 2012. Temperature sensitivity of greenhouse gas production in wetland soils of different vegetation. Biogeochemistry 108, 77–90. https://doi.org/10.1007/s10533-011-9573-3.

Jacotot, A., Marchand, C., Allenbach, M., 2018. Tidal variability of CO2 and CH4 emissions from the water column within a Rhizophora mangrove forest (New Caledonia). Sci. Total Environ. 631–632, 334–340. https://doi.org/10.1016/j.scitotenv.2018.03.006.

Johnston, H., Kinnison, D., 1998. Methane photooxidation in the atmosphere: contrast between two methods of analysis. J. Geophys. Res.-Atmos. 103, 21967–21984. https://doi.org/10.1029/98JD01213.

Katayama, A., Kume, T., Komatsu, H., Ohashi, M., Nakagawa, M., Yamashita, M., Otsuki, K., Suzuki, M., Kumagai, T., 2009. Effect of forest structure on the spatial variation in soil respiration in a Bornean tropical rainforest. Agric. For. Meteorol. 149, 1666–1673. https://doi.org/10.1016/j.agrformet.2009.05.007.

Keeling, C.D., 1958. The concentration and isotopic abundances of atmospheric carbon dioxide in rural areas. Geochim. Cosmochim. Acta 13, 322–334.
Keeling, C.D., 1961. The concentration and isotopic abundances of carbon dioxide in rural and marine air. Geochim. Cosmochim. Acta 24, 277–298. https://doi.org/10.1016/0016-7037(61)90023-0.
Khan, N.S., Vane, C.H., Horton, B.P., 2015. Stable carbon isotope and C/N geochemistry of coastal wetland sediments as a sea-level indicator. Handb. Sea-Level Res. 295–311.
Kirui, B., Huxham, M., Kairo, J., Mencuccini, M., Skov, 2009. Seasonal dynamics of soil carbon dioxide flux in a restored young mangrove plantation at Gazi Bay. Adv. Coast. Ecol. 20, 122–130.
Kreuzwieser, J., Buchholz, J., Rennenberg, H., 2003. Emission of methane and nitrous oxide by Australian mangrove ecosystems. Plant Biol. 5, 423–431.
Kristensen, E., Bouillon, S., Dittmar, T., Marchand, C., 2008. Organic carbon dynamics in mangrove ecosystems: a review. Aquat. Bot. 89, 201–219. https://doi.org/10.1016/j.aquabot.2007.12.005.
Lamb, A.L., Wilson, G.P., Leng, M.J., 2006. A review of coastal palaeoclimate and relative sea-level reconstructions using δ13C and C/N ratios in organic material. Earth-Sci. Rev. 75, 29–57. https://doi.org/10.1016/j.earscirev.2005.10.003.
Lee, S.Y., Primavera, J.H., Dahdouh-Guebas, F., McKee, K., Bosire, J.O., Cannicci, S., Diele, K., Fromard, F., Koedam, N., Marchand, C., Mendelssohn, I., Mukherjee, N., Record, S., 2014. Ecological role and services of tropical mangrove ecosystems: a reassessment. Glob. Ecol. Biogeogr. 23, 726–743. https://doi.org/10.1111/geb.12155.
Leopold, A., Marchand, C., Deborde, J., Chaduteau, C., Allenbach, M., 2013. Influence of mangrove zonation on CO 2 fluxes at the sediment–air interface (New Caledonia). Geoderma 202, 62–70.
Leopold, A., Marchand, C., Deborde, J., Allenbach, M., 2015. Temporal variability of CO 2 fluxes at the sediment-air interface in mangroves (New Caledonia). Sci. Total Environ. 502, 617–626.
Lin, G., Ehleringer, J.R., 1997. Carbon isotopic fractionation does not occur during dark respiration in C3 and C4 plants. Plant Physiol. 114, 391–394. https://doi.org/10.1104/pp.114.1.391.
Litton, C.M., Giardina, C.P., Albano, J.K., Long, M.S., Asner, G.P., 2011. The magnitude and variability of soil-surface CO2 efflux increase with mean annual temperature in Hawaiian tropical montane wet forests. Soil Biol. Biochem. 43, 2315–2323. https://doi.org/10.1016/j.soilbio.2011.08.004.
Livesley, S.J., Andrusiak, S.M., 2012. Temperate mangrove and salt marsh sediments are a small methane and nitrous oxide source but important carbon store. Estuar. Coast. Shelf Sci. 97, 19–27. https://doi.org/10.1016/j.ecss.2011.11.002.
Lloyd, J., Taylor, J., 1994. On the temperature dependence of soil respiration. Funct. Ecol. 83, 315–323.
Lou, Y.-S., Li, Z.-P., Zhang, T.-L., 2003. Soil CO2 flux in relation to dissolved organic carbon, soil temperature and moisture in a subtropical arable soil of China. J. Environ. Sci. (China) 15, 715–720.
Lovelock, C.E., 2008. Soil respiration and belowground carbon allocation in mangrove forests. Ecosystems 11, 342–354. https://doi.org/10.1007/s10021-008-9125-4.
Lüthi, D., Le Floch, M., Bereiter, B., Blunier, T., Barnola, J.-M., Siegenthaler, U., Raynaud, D., Jouzel, J., Fischer, H., Kawamura, K., Stocker, T.F., 2008. High-resolution carbon dioxide concentration record 650,000–800,000 years before present. Nature 453, 379–382. https://doi.org/10.1038/nature06949.
Lyimo, T.J., Pol, A., Op den Camp, H.J.M., 2002. Sulfate reduction and methanogenesis in sediments of Mtoni Mangrove Forest, Tanzania. AMBIO J. Hum. Environ. 31, 614–616. https://doi.org/10.1579/0044-7447-31.7.614.
Mackey, A.P., Smail, G., 1996. The decomposition of mangrove litter in a subtropical mangrove forest. Hydrobiologia 332, 93–98. https://doi.org/10.1007/BF00016688.
Maher, D.T., Cowley, K., Santos, I.R., Macklin, P., Eyre, B.D., 2015. Methane and carbon dioxide dynamics in a subtropical estuary over a diel cycle: insights from automated in situ radioactive and stable isotope measurements. Mar. Chem. 168, 69–79. https://doi.org/10.1016/j.marchem.2014.10.017.
Marchand, C., Lallier-Vergès, E., Allenbach, M., 2011. Redox conditions and heavy metals distribution in mangrove forests receiving effluents from shrimp farms (Teremba Bay, New Caledonia). J. Soils Sediments 11, 529–541. https://doi.org/10.1007/s11368-010-0330-3.
McLeod, E., Chmura, G.L., Bouillon, S., Salm, R., Björk, M., Duarte, C.M., Lovelock, C.E., Schlesinger, W.H., Silliman, B.R., 2011. A blueprint for blue carbon: toward an improved understanding of the role of vegetated coastal habitats in sequestering CO_2. Front. Ecol. Environ. 9, 552–560. https://doi.org/10.1890/110004.
Metcalfe, D., Meir, P., Aragao, L.E.O.C., Malhi, Y., Costa, D., L, A.C., Braga, A., Goncalves, P.H.L., de Athaydes, J., Almeida, D., S., S., Williams, M., 2007. Factors controlling spatio-temporal variation in carbon dioxide efflux from surface litter, roots, and soil organic matter at four rain forest sites in the eastern Amazon. J. Geophys. Res. 112, 04001. https://doi.org/10.1029/2007JG000443.
Moore, T.R., Knowles, R., 1990. Methane emissions from fen, bog and swamp peatlands in Quebec. Biogeochemistry 11, 45–61.
Myhre, G., Shindell, D., Bréon, F.-M., Collins, W., Fuglestvedt, J., Huang, J., Koch, D., Lamarque, J.-F., Lee, D., Mendoza, B., 2013. Others, 2013. Anthropogenic and natural radiative forcing. Clim. Change. Phys. Sci. Basis Contrib. Work. Group Fifth Assess. Rep. Intergov. Panel Clim. Change Stock. TF Qin G-K Plattner M Tignor SK Allen J Boschung Nauels Xia V Bex PM Midgley Eds 423, 658–740.
Oertel, C., Matschullat, J., Zurba, K., Zimmermann, F., Erasmi, S., 2016. Greenhouse gas emissions from soils—a review. Chem. Erde-Geochem. 76, 327–352. https://doi.org/10.1016/j.chemer.2016.04.002.
O'Leary, M.H., 1988. Carbon isotopes in photosynthesis. Bioscience 38, 328–336.
Parkin, T.B., Kaspar, T.C., 2003. Temperature controls on diurnal carbon dioxide flux. Soil Sci. Soc. Am. J. 67, 1763–1772. https://doi.org/10.2136/sssaj2003.1763.
Pataki, D.E., Ehleringer, J.R., Flanagan, L.B., Yakir, D., Bowling, D.R., Still, C.J., Buchmann, N., Kaplan, J.O., Berry, J.A., 2003. The application and interpretation of Keeling plots in terrestrial carbon cycle research. Glob. Biogeochem. Cycles 17.
Poungparn, S., Komiyama, A., Tanaka, A., Sangtiean, T., Maknual, C., Kato, S., Tanapermpool, P., Patanaponpaiboon, P., 2009. Carbon dioxide emission through soil respiration in a secondary mangrove forest of eastern Thailand. J. Trop. Ecol. 25, 393–400.
R Development Core Team, 2008. R: A Language and Environment for Statistical Computing. R Foundation for Statistical Computing, Vienna, Austria.
Raich, J.W., Schlesinger, W.H., 1992. The global carbon dioxide flux in soil respiration and its relationship to vegetation and climate. Tellus Ser. B Chem. Phys. Meteorol. B 44, 81–99. https://doi.org/10.1034/j.1600-0889.1992.t01-1-00001.x.
Segers, R., 1998. Methane production and methane consumption: a review of processes underlying wetland methane fluxes. Biogeochemistry 41, 23–51.
Sjögersten, S., Black, C.R., Evers, S., Hoyos-Santillan, J., Wright, E.L., Turner, B.L., 2014. Tropical wetlands: a missing link in the global carbon cycle? Glob. Biogeochem. Cycles 28, 1371–1386. https://doi.org/10.1002/2014GB004844.
Sun, Z., Jiang, H., Wang, L., Mou, X., Sun, W., 2013. Seasonal and spatial variations of methane emissions from coastal marshes in the northern Yellow River estuary, China. Plant Soil 369, 317–333. https://doi.org/10.1007/s11104-012-1564-1.
Trudeau, N.C., Garneau, M., Pelletier, L., 2013. Methane fluxes from a patterned fen of the northeastern part of the La Grande river watershed, James Bay, Canada. Biogeochemistry 113, 409–422. https://doi.org/10.1007/s10533-012-9767-3.
Turetsky, M.R., Treat, C.C., Waldrop, M.P., Waddington, J.M., Harden, J.W., McGuire, A.D., 2008. Short-term response of methane fluxes and methanogen activity to water table and soil warming manipulations in an Alaskan peatland. J. Geophys. Res. Biogeosci. 113, G00A10. https://doi.org/10.1029/2007JG000496.
Virly, S., 2006. Virly. 2008, Typologies et Biodiversité des mangroves Rapport_Mangroves_ZoNeCo_2006_2007.pdf.
Wang, C., Lai, D.Y.F., Tong, C., Wang, W., Huang, J., Zeng, C., 2015. Variations in temperature sensitivity (Q10) of CH4 emission from a subtropical estuarine marsh in Southeast China. PLoS One 10. https://doi.org/10.1371/journal.pone.0125227.
Wang, H., Liao, G., D'Souza, M., Yu, X., Yang, J., Yang, X., Zheng, T., 2016. Temporal and spatial variations of greenhouse gas fluxes from a tidal mangrove wetland in Southeast China. Environ. Sci. Pollut. Res. 23, 1873–1885. https://doi.org/10.1007/s11356-015-5440-4.
Xu, M., Qi, Y., 2001. Soil-surface CO2 efflux and its spatial and temporal variations in a young ponderosa pine plantation in northern California. Glob. Chang. Biol. 7, 667–677. https://doi.org/10.1046/j.1354-1013.2001.00435.x.
Yentsch, C.S., Menzel, D.W., 1963. A method for the determination of phytoplankton chlorophyll and phaeophytin by fluorescence. Deep Sea Research and Oceanographic Abstracts. Elsevier, pp. 221–231.
Zeebe, R.E., Ridgwell, A., Zachos, J.C., 2016. Anthropogenic carbon release rate unprecedented during the past 66 million years. Nat. Geosci. 9. https://doi.org/10.1038/ngeo2681 ngeo2681.